

New Catalytic Systems Used for Wastewater Treatment [†]

Cristina-Emanuela Enascuta ¹, Elena-Emilia Sirbu ^{1,2,*}, Radu Claudiu Fierascu ¹, Diana Pasarin ¹, Andra-Ionela Ghizdareanu ¹, Grigore Psenovschi ^{1,3} and Mihaela Ganciarov ¹

¹ National Institute for Research & Development in Chemistry and Petrochemistry—ICECHIM, 202 Splaiul Independentei, 060021 Bucharest, Romania; cristina.enascuta@gmail.com (C.-E.E.); radu_claudiu_fierascu@yahoo.com (R.C.F.); diana.pasarin@gmail.com (D.P.); gregorypshehovschi@gmail.com (G.P.); mihaela.ganciarov@icechim.ro (M.G.)

² Chemistry Department, Petroleum Gas University of Ploiești, Bucharest Blvd 39, 100680 Ploiești, Romania

³ Doctoral School, National University of Science and Technology Politehnica of Bucharest, Splaiul Independentei No. 313, 060042 Bucharest, Romania

* Correspondence: oprescuemilia@gmail.com

[†] Presented at the 19th International Symposium “Priorities of Chemistry for a Sustainable Development”, Bucharest, Romania, 11–13 October 2023.

Abstract: Annually, considerable amounts of polluted water are produced due to industrialization based on processing in various industries. The purpose of this study refers to a process of obtaining a photocatalytic system with a structure of metal oxides in the field of ultrasound, used in the advanced treatment of wastewater resulting from the pharmaceutical and agricultural industries. These photocatalytic systems allow wastewater to be treated in a relatively short time, being quickly recovered and reused repeatedly. To quantify the efficiency of the photocatalyst in treating wastewater, experiments were carried out in the presence of sunlight, in the absence and presence of the photocatalyst, with a methylene blue solution.

Keywords: photocatalysts; wastewater treatment; ultrasound field



Citation: Enascuta, C.-E.; Sirbu, E.-E.; Fierascu, R.C.; Pasarin, D.; Ghizdareanu, A.-I.; Psenovschi, G.; Ganciarov, M. New Catalytic Systems Used for Wastewater Treatment. *Chem. Proc.* **2023**, *13*, 19. <https://doi.org/10.3390/chemproc2023013019>

Academic Editors: Mihaela Doni and Florin Oancea

Published: 23 November 2023



Copyright: © 2023 by the authors. Licensee MDPI, Basel, Switzerland. This article is an open access article distributed under the terms and conditions of the Creative Commons Attribution (CC BY) license (<https://creativecommons.org/licenses/by/4.0/>).

1. Introduction

Wastewater contaminated with various toxic compounds is a global environmental problem. These compounds from the pharmaceutical industry or agriculture are frequently detected in water resources around the world, proving to be harmful to human health and even the entire ecosystem [1]. A huge amount of polluted water is also produced annually due to industrialization based on processing in various industries, such as pharmaceutical, textile, food, agricultural, petrochemical, etc. [2]. Over the years, various conventional wastewater treatment methods, such as biological oxidation, carbon bed adsorption, membrane separation, electrochemical treatment, and oxidation, have been used. The limitations of these effective treatment methods have meant that the wastewater is not recycled, leading to the research of additional treatment methods, which creates additional stress on water availability [3]. It is a challenge for researchers to search for different ecological and economic strategies for wastewater treatment that can be used on an industrial scale [4]. Advanced wastewater oxidation processes represent promising and ecological solutions capable of mineralizing harmful substances. In recent years, the semiconducting properties of metal oxides and their use in photocatalytic water treatment have been widely studied [5]. Photocatalysts, especially those based on titanium dioxide (TiO₂) or zinc oxide (ZnO), are intensively studied due to their high chemical stability, promising efficiency, low cost, excellent photocatalytic activity, and non-toxicity, leading to their use in the water treatment process [6]. Due to the short carrier diffusion path along the walls leading to rapid mass transfer of reactants, TiO₂-based catalysts are efficient photocatalysts [7]. Therefore, their optimal size is a necessity for their successful application in pollutant removal. TiO₂ does not produce toxins during degradation, which makes it

sustainable and, therefore, preferable. The use of ultrasound to obtain photocatalysts based on metal oxides has significant potential to improve the synthesis of nanoparticles, due to the relatively easy applicability and the cavitation effects that can improve the synthesis process, with time and ultrasound power being the important parameters in obtaining nanomaterials with optimal and uniform dimensions [8,9].

In this context, the aim of this study refers to a process for obtaining, in the ultrasound field, a photocatalytic system with the structure of metal oxides used in the advanced treatment of wastewater resulting from the pharmaceutical and agriculture industries.

2. Materials and Methods

2.1. Materials

All the substances used to obtain the catalytic systems were of high purity and purchased from Sigma-Aldrich (Darmstadt, Germany) and Scharlau (Barcelona, Spain). The magnetic photocatalyst containing oxide components of Fe_2O_3 , TiO_2 , and La_2O_3 was obtained from the co-precipitation–calcination method [10]. A layer of iron oxide is deposited over the mixture of titanium dioxide and lanthanum. The new photocatalytic system can be activated in the presence of sunlight, being used to treat wastewater with organic compounds from the pharmaceutical industry or agricultural waters. The new catalysts were characterized using modern identification methods, such as XRD, FTIR, and SEM analysis.

2.2. Catalyst Preparation

The photocatalytic system was obtained via the co-precipitation–calcination method of the following salts: LaCl_3 , TiCl_4 , and FeCl_3 in an ultrasound field.

The experiment was carried out in a reaction vessel under an ultrasound field, where LaCl_3 (0.06 g) was dissolved in distilled water. Distilled water (90 mL) and ice were added to the mixture and kept under the ultrasonic field for 15 min. TiCl_4 (3.9 g) is added dropwise to the ice bath until the ice melts completely. We continued to add NH_4OH until pH-7.5. The mixture was kept under stirring for 30 min. The catalytic system based on TiO_2 was washed with distilled water until pH-6. The photocatalyst was centrifuged and dried at 100 °C for 10 h and calcined at 450 °C for 3 h.

$\text{TiO}_2\text{-La}_2\text{O}_3$ (2.5 g) is dissolved in distilled water (60 mL) under an ultrasound field for 10 min. Add FeCl_3 (4.5 g) for 15 min at room temperature and NH_4OH until pH-7.5. The formed mixture is kept under the ultrasound field for 30 min at a temperature of 25–30 °C. The photocatalyst is washed with distilled water until pH-6. The resulting mixture is centrifuged and dried at 100 °C for 10 h and calcined at 450 °C for 3 h.

2.3. Catalyst Characterization

X-ray diffraction (XRD) analyses were performed using the Bruker D8 Advance X-ray diffractometer with $\text{CuK}\alpha$ radiation ($k\text{Cu} = 1.5406 \text{ \AA}$) operated at 40 kV and 40 mA. Data were collected in the 2θ range from 10.0° to 80°, with a scan rate of 0.2 degrees/min.

The FTIR analysis of the samples was performed in the attenuated total reflection (ATR) mode, with a Perkin Elmer Spectrum GX spectrometer (Waltham, MA, USA) in the range 4000–600 cm^{-1} , with 32 scans and a resolution of 4 cm^{-1} .

Surface morphology and cross-sectional microstructures were visualized using SEM characterization with a Hitachi TM4000 plus II (Tokyo, Japan) equipped with an ESB detector and vacuum conductor at an accelerating voltage of 5–15 kV.

2.4. Photocatalytic Degradation Preliminary Tests

The preliminary tests regarding photocatalytic degradation of the methylene blue (MB) were performed in Erlenmeyer flasks. The MB solution of known concentration together with the catalytic system was left in UV sunlight for 72 h. To quantify the contribution of the photocatalyst, the experiments were performed in the presence of sunlight in the absence and presence of the catalyst with a methylene blue solution.

3. Results and Discussion

Catalyst Characterization

The presence of existing groups in the structure of the obtained photocatalysts can also be identified in the FTIR spectra. For $\text{Fe}_2\text{O}_3\text{-TiO}_2\text{-La}_2\text{O}_3$ (Figure 1B), we can observe the characteristic peaks of Fe(II)-O groups at the wavelengths 445 cm^{-1} , 474 cm^{-1} , and 542 cm^{-1} ; for Fe(III)-O groups, we can observe the vibrations at 418 cm^{-1} and 457 cm^{-1} , and the Ti-O groups are found at the wavelengths 429 cm^{-1} , 587 cm^{-1} and 669 cm^{-1} .

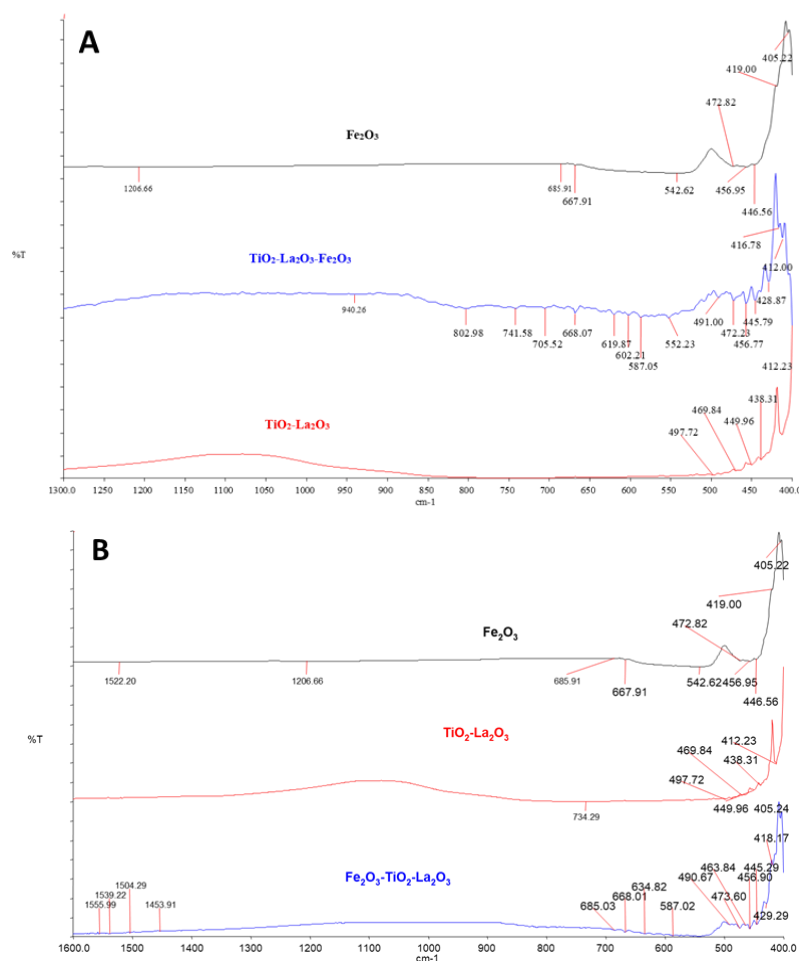


Figure 1. The FT-IR spectra of $\text{TiO}_2\text{-La}_2\text{O}_3\text{-Fe}_2\text{O}_3$ (A) and $\text{Fe}_2\text{O}_3\text{-TiO}_2\text{-La}_2\text{O}_3$ (B).

In the case of $\text{TiO}_2\text{-La}_2\text{O}_3\text{-Fe}_2\text{O}_3$ (Figure 1B), the characteristic peaks of the Fe(II)-O groups can be observed at the wavelengths 446 cm^{-1} , 472 cm^{-1} , and 542 cm^{-1} ; for the Fe(III)-O groups, the vibrations can be observed at 416 cm^{-1} and 456 cm^{-1} , and the Ti-O groups are found at the wavelengths 429 cm^{-1} , 587 cm^{-1} , and 668 cm^{-1} .

The crystal structures for $\text{TiO}_2\text{-La}_2\text{O}_3\text{-Fe}_2\text{O}_3$ and $\text{Fe}_2\text{O}_3\text{-TiO}_2\text{-La}_2\text{O}_3$ were investigated via X-ray diffraction analysis (Figure 2).

The XRD diffractogram of the photocatalysts (Figure 1) indicates the presence of peaks corresponding to the hematite crystallization form related to Fe_2O_3 and TiO_2 peaks that can be attributed to the anatase crystallization form.

The XRD diffractogram of $\text{Fe}_2\text{O}_3\text{-TiO}_2\text{-La}_2\text{O}_3$ indicates the presence of peaks corresponding to the hematite crystallization form related to Fe_2O_3 at 2θ angles of 24.10° (012); 33.14° (104); 35.62° (110); 40.85° (113); 49.47° (024); 54.06° (116); 57.52° (122); 64.12° (300); 71.88° (1010); 81.23° (312); 83.04° (0210); 84.99° (134); and 88.69° (226). Peaks of TiO_2 can be attributed to the anatase crystallization form (2θ angles of 25.29° (101); 37.95° (004); 43.17° (400); 48.19° (200); 68.10° (116); 79.12° (206)) [11]. For $\text{TiO}_2\text{-La}_2\text{O}_3\text{-Fe}_2\text{O}_3$, the XRD analysis

shows peaks only for the crystallization forms hematite and anatase, corresponding to metal oxides based on Fe and Ti. It should be mentioned that, with both photocatalysts, no peaks characteristic of the crystalline phase of lanthanum oxide were observed at 2θ angles of 27.36° , 39.62° , and 48.69° , suggesting the integration of lanthanum oxide in the crystalline network of titanium dioxide [12].

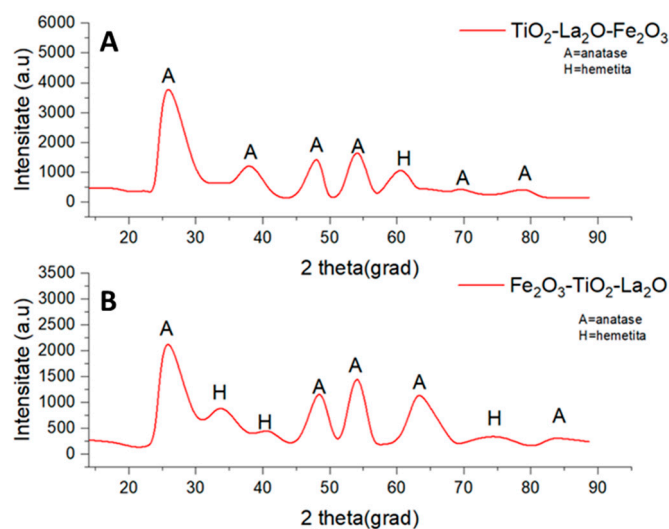


Figure 2. X-ray diffraction analysis of $\text{TiO}_2\text{-La}_2\text{O-Fe}_2\text{O}_3$ (A) and $\text{Fe}_2\text{O}_3\text{-TiO}_2\text{-La}_2\text{O}$ (B).

The SEM images suggest an agglomerated morphology with a certain porosity for the $\text{Fe}_2\text{O}_3\text{-TiO}_2\text{-La}_2\text{O}$ and $\text{TiO}_2\text{-La}_2\text{O-Fe}_2\text{O}_3$ catalysts (Figure 3).

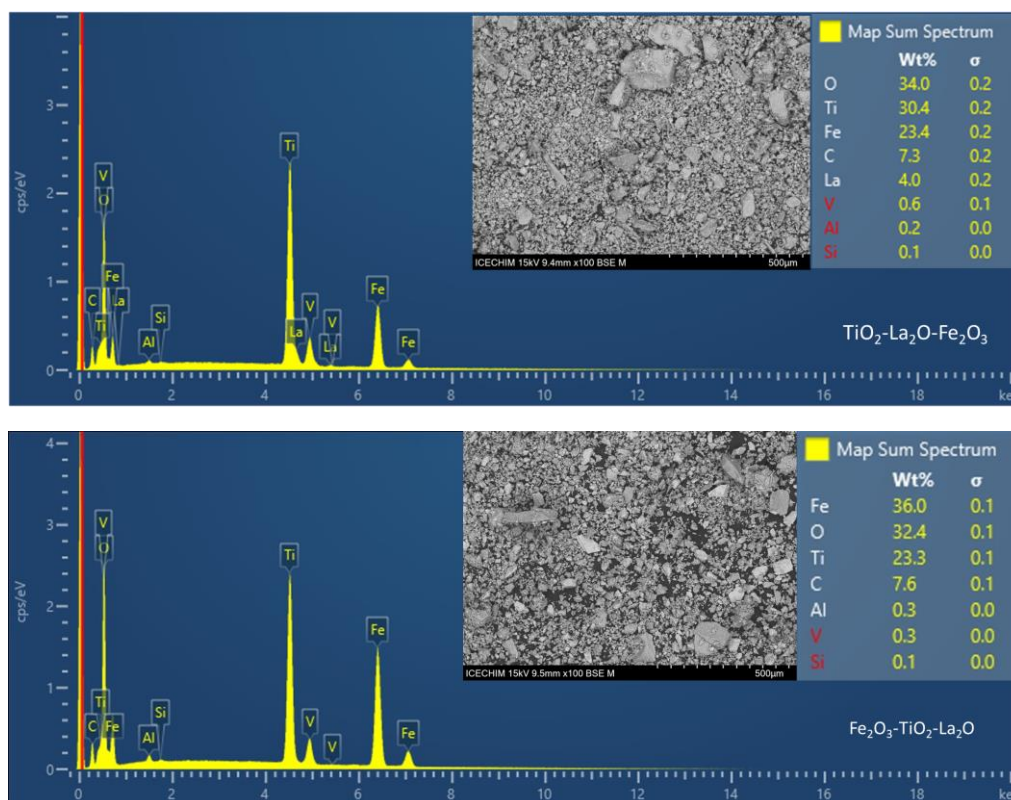


Figure 3. Surface morphology of $\text{TiO}_2\text{-La}_2\text{O-Fe}_2\text{O}_3$ and $\text{Fe}_2\text{O}_3\text{-TiO}_2\text{-La}_2\text{O}$.

The EDX spectrum confirms the majority presence of Fe, Ti, C, La, and O. For example, for the $\text{TiO}_2\text{-La}_2\text{O}_3\text{-Fe}_2\text{O}_3$ photocatalyst, the Ti content was 30.4%, followed by Fe 23.4% and, respectively, 4% La. But, in the case of the $\text{Fe}_2\text{O}_3\text{-TiO}_2\text{-La}_2\text{O}_3$ photocatalyst, the Fe content was 36%, while the Ti content decreased to 23.3%, and the La presence disappeared, which is consistent with the XRD analyses.

The irradiation time and the adsorption balance between the photocatalyst and the MB solution represent the most important parameters that control the photodegradation. Samples were taken every 12 h, and the absorbance was read. It was observed that the absorption peak of the MB spectra gradually decreases with the increase in the irradiation time and then becomes constant. A decrease in color intensity from blue to colorless was observed after approximately 72 h.

As can be seen in Figure 4, the MB removal increases with irradiation time, from 19.8 and 23.54%, after 12 h, to maximum values of 92.5% and 98.45%, after 72 h, for the $\text{Fe}_2\text{O}_3\text{-TiO}_2\text{-La}_2\text{O}_3$ and $\text{TiO}_2\text{-La}_2\text{O}_3\text{-Fe}_2\text{O}_3$ photocatalysts, respectively. This behavior is in agreement with the data presented by Khan I. et al. [13]. The highest degradation efficiency, after 48 h, was observed for the $\text{TiO}_2\text{-La}_2\text{O}_3\text{-Fe}_2\text{O}_3$ photocatalyst with an 85.74% MB removal, compared with $\text{Fe}_2\text{O}_3\text{-TiO}_2\text{-La}_2\text{O}_3$ of only 62.84% MB removal.

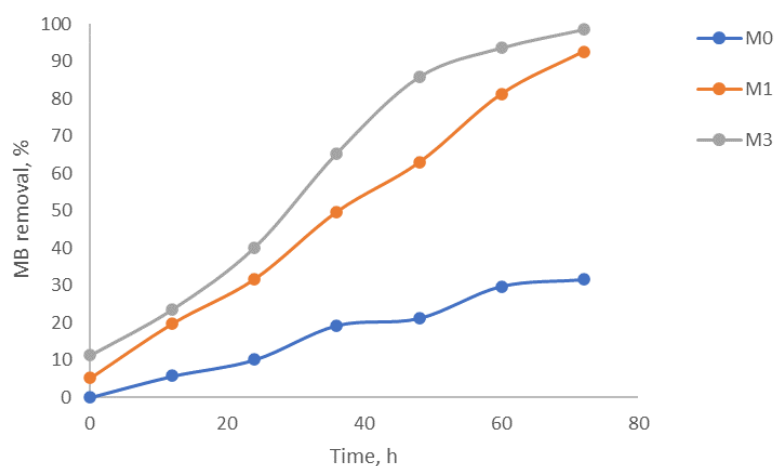


Figure 4. MB Methylene blue degradation over time, M0 (without photocatalyst), M1 ($\text{Fe}_2\text{O}_3\text{-TiO}_2\text{-La}_2\text{O}_3$), M3 ($\text{TiO}_2\text{-La}_2\text{O}_3\text{-Fe}_2\text{O}_3$).

These results can be explained by the highest Ti content of 30.4% contained in the $\text{TiO}_2\text{-La}_2\text{O}_3\text{-Fe}_2\text{O}_3$ photocatalyst.

4. Conclusions

The photocatalytic systems based on oxide components of Fe_2O_3 , TiO_2 , and La_2O_3 were obtained via the co-precipitation–calcination method in the presence of the ultrasound-assisted field. These systems allow wastewater to be treated in a relatively short time, quickly recovered, and reused repeatedly. Thus, the amount of photocatalyst and its reuse, as well as the time of exposure to sunlight, are some of the most important parameters in the successful implementation of the entire wastewater treatment process. In order to quantify the contribution of the photocatalyst to the wastewater treatment, experiments were carried out in the presence of sunlight in the absence and presence of the photocatalyst with a methylene blue solution.

Author Contributions: Conceptualization, C.-E.E. and E.-E.S.; methodology C.-E.E., E.-E.S. and R.C.F.; software, A.-I.G.; validation, D.P. and M.G.; formal analysis, R.C.F. and M.G.; investigation, C.-E.E. and E.-E.S.; resources, D.P. and R.C.F.; data curation, G.P.; writing—original draft preparation, C.-E.E. and E.-E.S.; writing—review and editing, C.-E.E. and E.-E.S.; supervision, C.-E.E.; project administration, R.C.F. All authors have read and agreed to the published version of the manuscript.

Funding: This research was funded by the Ministry of Research, Innovation and Digitization through Program 1—Development of the national research-development system, Subprogram 1.2—Institutional performance—Projects to finance excellence in RDI, Contract no. 15PFE/2021. This work was carried out through the PN 23.06 Core Program—ChemNewDeal within the National Plan for Research, Development and Innovation 2022–2027, developed with the support of the Ministry of Research, Innovation, and Digitization, project no. PN 23.06.01.01 (AQUAMAT).

Institutional Review Board Statement: Not applicable.

Informed Consent Statement: Not applicable.

Data Availability Statement: Data are contained within the article.

Conflicts of Interest: The authors declare no conflict of interest.

References

1. Zhang, S.; Wang, J.; Zhang, Y.; Ma, J.; Huang, L.; Yu, S.; Chen, L.; Song, G.; Qiu, M.; Wang, X. Applications of water-stable metal-organic frameworks in the removal of water pollutants: A review. *Environ. Pollut.* **2021**, *291*, 118076. [[CrossRef](#)] [[PubMed](#)]
2. Chandak, S.; Ghosh, P.K.; Gogate, P. Treatment of real pharmaceutical wastewater using different processes based on ultrasound in combination with oxidants. *Process Saf. Environ. Prot.* **2020**, *137*, 149–157. [[CrossRef](#)]
3. Meili, L.; Soletti, J. Electrochemical process and Fenton reaction followed by lamellar settler to oil/surfactant effluent degradation. *J. Water Process. Eng.* **2019**, *31*, 100841.
4. Sudhaik, A.; Raizada, P.; Khan, A.A.P.; Singh, A.; Singh, P. Graphitic carbon nitride-based upconversion photocatalyst for hydrogen production and water purification. *Nanofabrication* **2022**, *7*, 280–313. [[CrossRef](#)]
5. Kumar, A.; Raizada, P.; Singh, P.; Saini, R.V.; Saini, A.K.; Hosseini-Bandegharai, A. Perspective and status of polymeric graphitic carbon nitride-based Z-scheme photocatalytic systems for sustainable photocatalytic water purification. *Chem. Eng. J.* **2020**, *391*, 123496. [[CrossRef](#)]
6. Chen, D.; Cheng, Y.; Zhou, N.; Chen, P.; Wang, Y.; Li, K. Photocatalytic degradation of organic pollutants using TiO₂-based photocatalysts: A review. *J. Clean. Prod.* **2020**, *268*, 121725. [[CrossRef](#)]
7. Macak, J.M.; Zlamal, M.; Krysa, J.; Schmuki, P. Self-organized TiO₂ nanotube layers as highly efficient photocatalysts. *Small* **2007**, *2*, 300–304. [[CrossRef](#)] [[PubMed](#)]
8. Tiple, A.; Sinhmar, P.S.; Gogate, P.R. Improved direct synthesis of TiO₂ catalyst using sonication and its application for the desulfurization of thiophene. *Ultrason. Sonochem.* **2021**, *73*, 105547. [[CrossRef](#)] [[PubMed](#)]
9. Pinjari, D.V.; Prasad, K.; Gogate, P.R.; Mhaske, S.T.; Pandit, A.B. Synthesis of titanium dioxide by ultrasound assisted sol-gel technique: Effect of calcination and sonication time. *Ultrason. Sonochem.* **2015**, *23*, 185–191. [[CrossRef](#)] [[PubMed](#)]
10. Enascuta, C.-E.; Sirbu, E.-E.; Fierascu, R.C.; Ganciarov, M.; Psenovschi, G.; Vlaicu, A. Catalytic System with the Structure of Metal Oxides for the Treatment of Traces of Waste Water Residues. Patent Application no. A0339, 29 June 2023.
11. Guijarro, C. Reforming of Tar Model Compounds Using Iron Catalysts. Degree Project in Chemical Engineering. Master's Thesis, KTH Royal Institute of Technology, Stockholm, Sweden, 2020.
12. Sudhagar, S.; Kumar, S.S.; Premkumar, I.I.; Vijayan, V.; Venkatesh, R.; Rajkumar, S.; Singh, M. UV- and visible-light-driven TiO₂/La₂O₃ and TiO₂/Al₂O₃ nanocatalysts: Synthesis and enhanced photocatalytic activity. *Appl. Phys. A* **2022**, *128*, 282. [[CrossRef](#)]
13. Khan, I.; Saeed, K.; Zekker, I.; Zhang, B.; Hendi, A.H.; Ahmad, A.; Ahmad, S.; Zada, N.; Ahmad, H.; Shah, L.A.; et al. Review on Methylene Blue: Its Properties, Uses, Toxicity and Photodegradation. *Water* **2022**, *14*, 242. [[CrossRef](#)]

Disclaimer/Publisher's Note: The statements, opinions and data contained in all publications are solely those of the individual author(s) and contributor(s) and not of MDPI and/or the editor(s). MDPI and/or the editor(s) disclaim responsibility for any injury to people or property resulting from any ideas, methods, instructions or products referred to in the content.